

## Supplementary Data

### Supplementary Figure Legends

#### Supplementary Figures 1-6

#### Supplementary Tables 1-3

### Supplementary Figure Legends:

Supplementary Figure 1. Detection of human IL-6 secreted in human IL-6 knock-in RAG2<sup>-/-</sup>  $\gamma_c$ <sup>-/-</sup> mice by LPS stimulation.

RAG2<sup>-/-</sup>  $\gamma_c$ <sup>-/-</sup> mice were *i.p.* injected with 20 $\mu$ g LPS and serum samples were collected before and 2 hours after injection. (a) Human IL-6 level in serum samples of LPS injected IL-6m/m, IL-6h/m and IL-6h/h RAG2<sup>-/-</sup>  $\gamma_c$ <sup>-/-</sup> mice. (b) Mouse IL-6 level in serum samples of LPS injected IL-6m/m, IL-6h/m and IL-6h/h RAG2<sup>-/-</sup>  $\gamma_c$ <sup>-/-</sup> mice. Horizontal bars indicate the respective mean frequencies.

Supplementary Figure 2. Engraftment of human IL-6 dependent MM cell line INA-6 and development of a novel model for MM bone disease.

(a) Comparison of growth of INA-6 cells in IL-6<sup>m/m</sup> versus IL-6<sup>h/h</sup> mice. (b)  $\mu$ CT showing lytic destruction of bone in mice injected with INA-6 cells or sham injection. Right panel shows trabecular bone volume/tissue volume in the injected mice. (c) Comparison of growth of INA6 cells in RAG2<sup>-/-</sup>  $\gamma_c$ <sup>-/-</sup> mice expressing human IL-6, human SIRP $\alpha$ , or both (RGS6) mice. (d) Comparison of growth of primary CD138<sup>+</sup> tumor cells in RGS6 mice versus MIS<sup>(KI)</sup>TRG6 mice.

Supplementary Figure 3. Engraftment of tumor in MIS<sup>(KI)</sup>TRG6 vs SCID-hu models.

(a) Validation of SCID-hu model with injected INA-6 GFP<sup>+</sup> MM cell line. (b) Comparison of serum human light chain restricted monoclonal antibodies ( $\mu$ g/ml) detected by ELISA in mice engrafted with pre-neoplastic patient cells. (c) Comparison of serum levels of human sIL-6R (pg/ml) detected by ELISA in INA-6 cell line engrafted mice.

Supplementary Figure 4. Strategy for sorting tumor cells for genomic analysis.

Supplementary Figure 5. LOH analysis showing focal amplification of chromosome 1

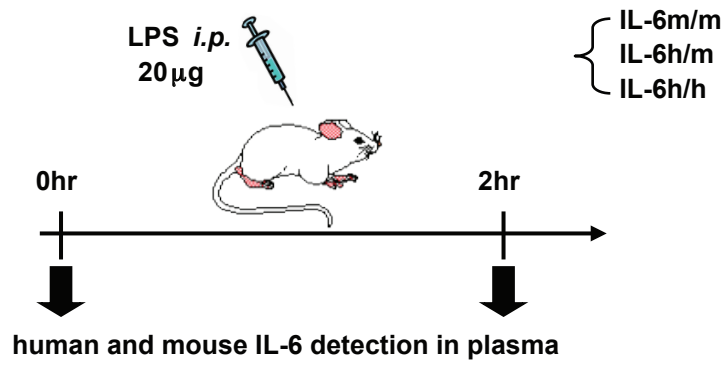
Supplementary Figure 6. Sanger sequencing showing the presence of a xenograft-emergent mutation in the matched baseline sample isolated from the patient.

Supplementary Table 1. Patient Characteristics.

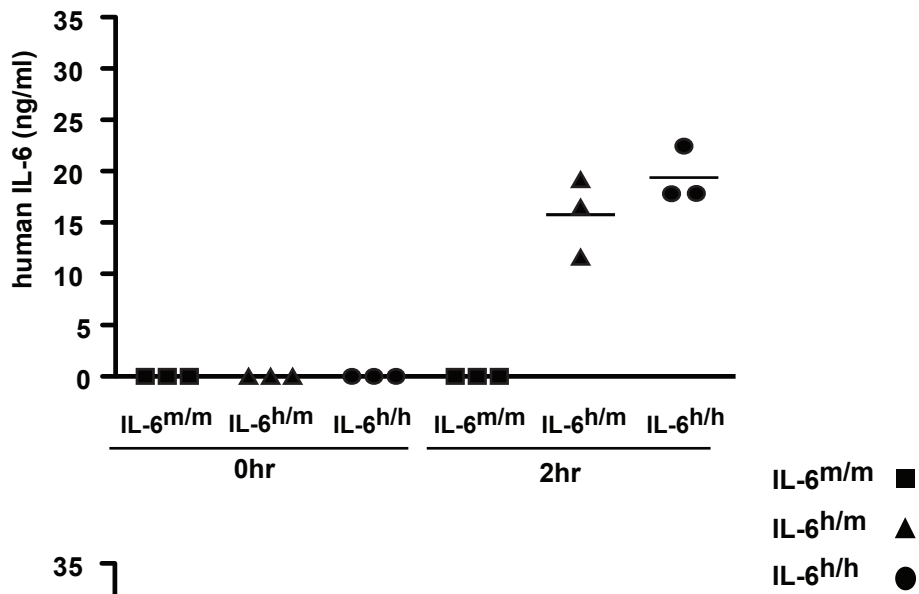
Supplementary Table 2. Summary statistics for whole exome sequencing analysis.

Supplementary Table 3. Source, clone and dilutions for antibodies.

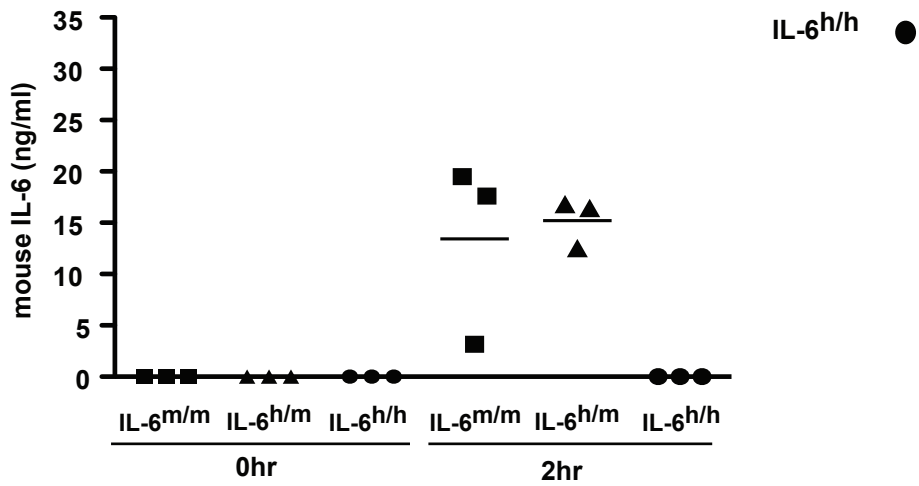
Supplementary Figure S1



a)

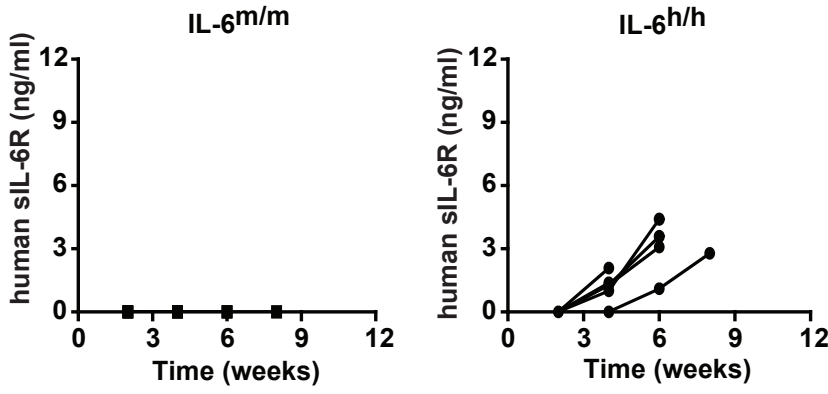


b)

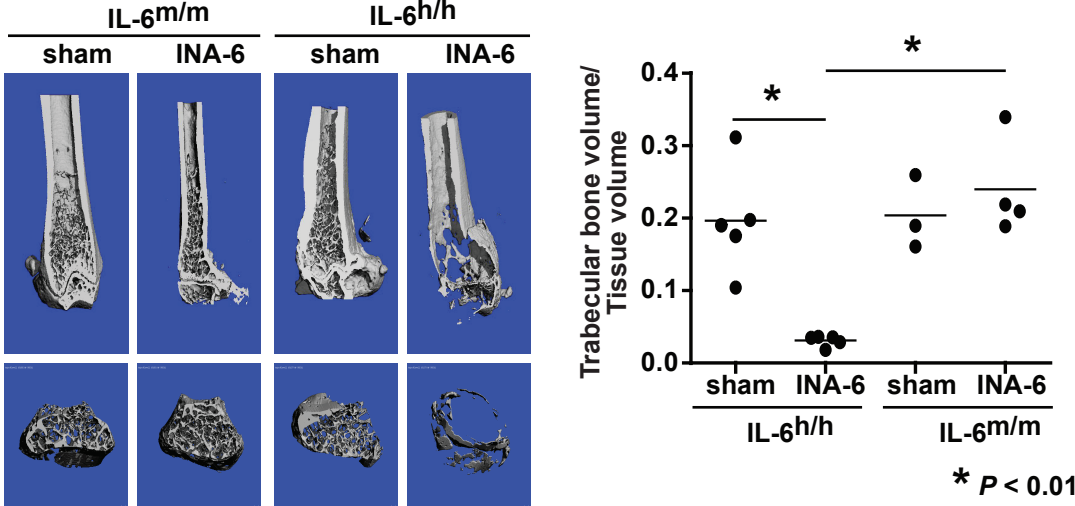


Supplementary Figure S2

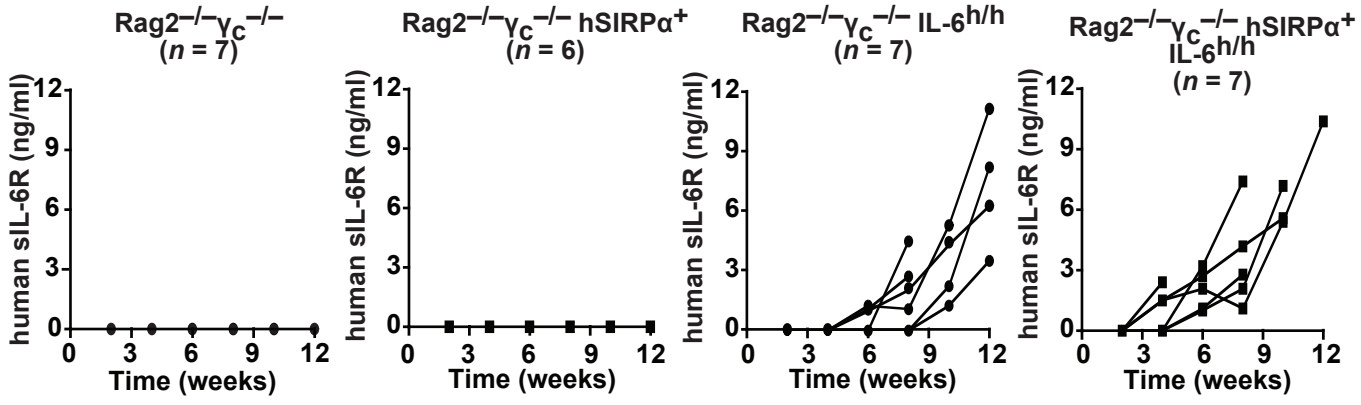
a)



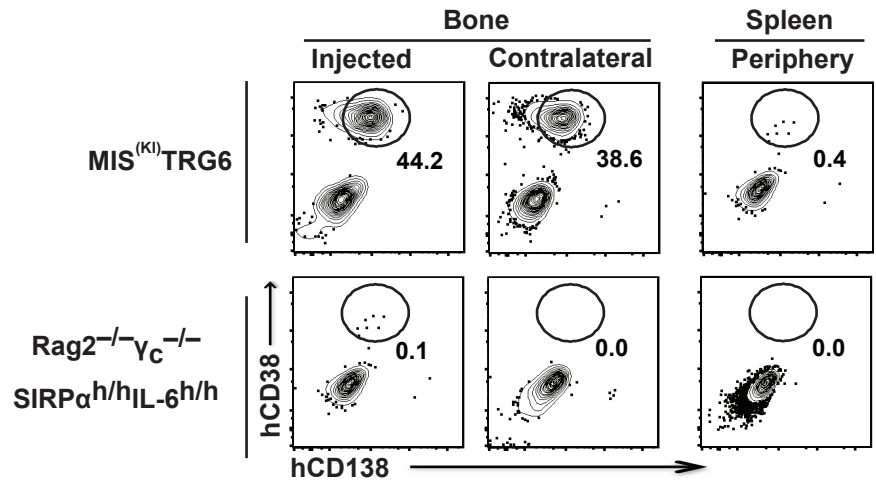
b)



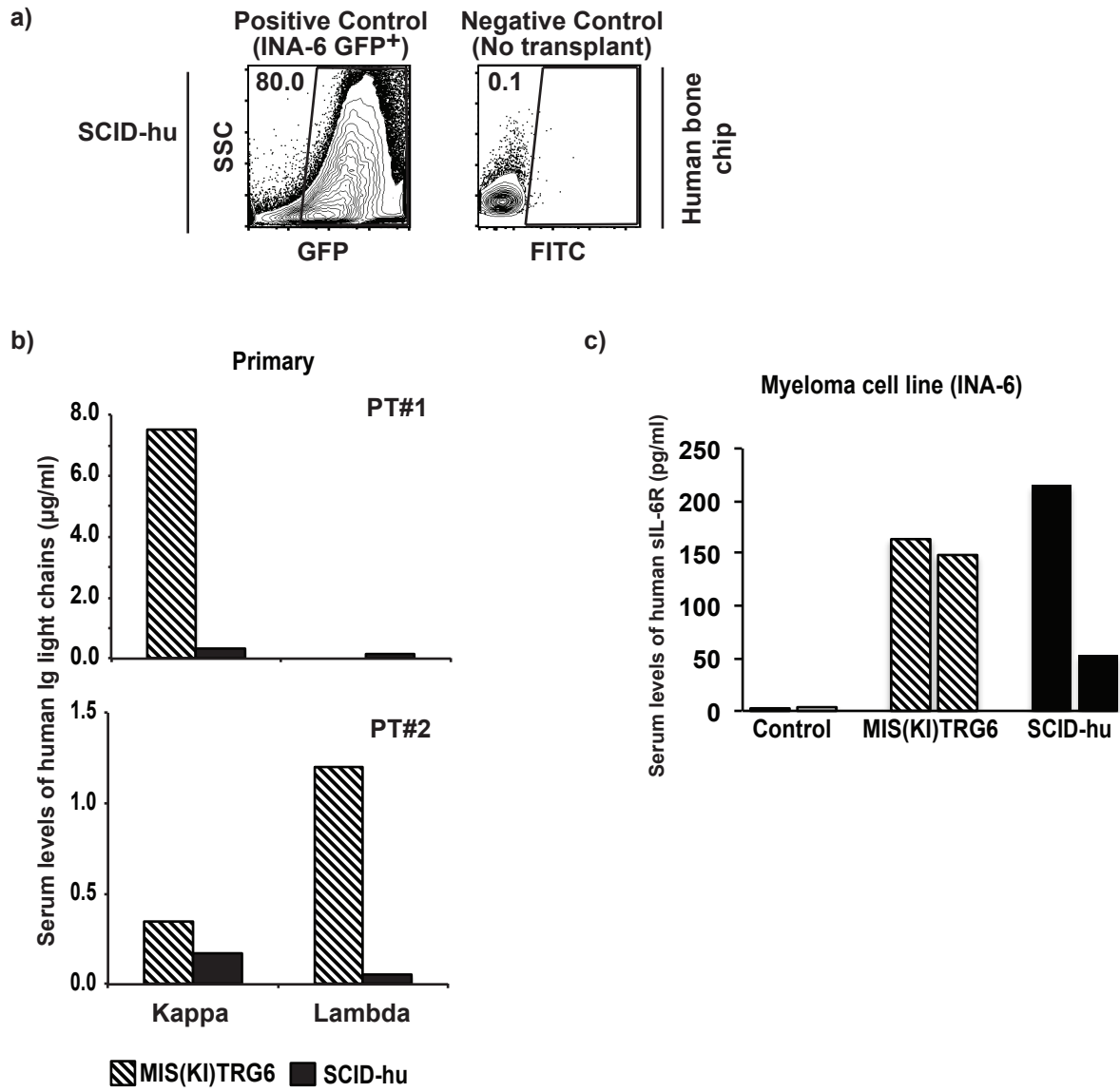
c)



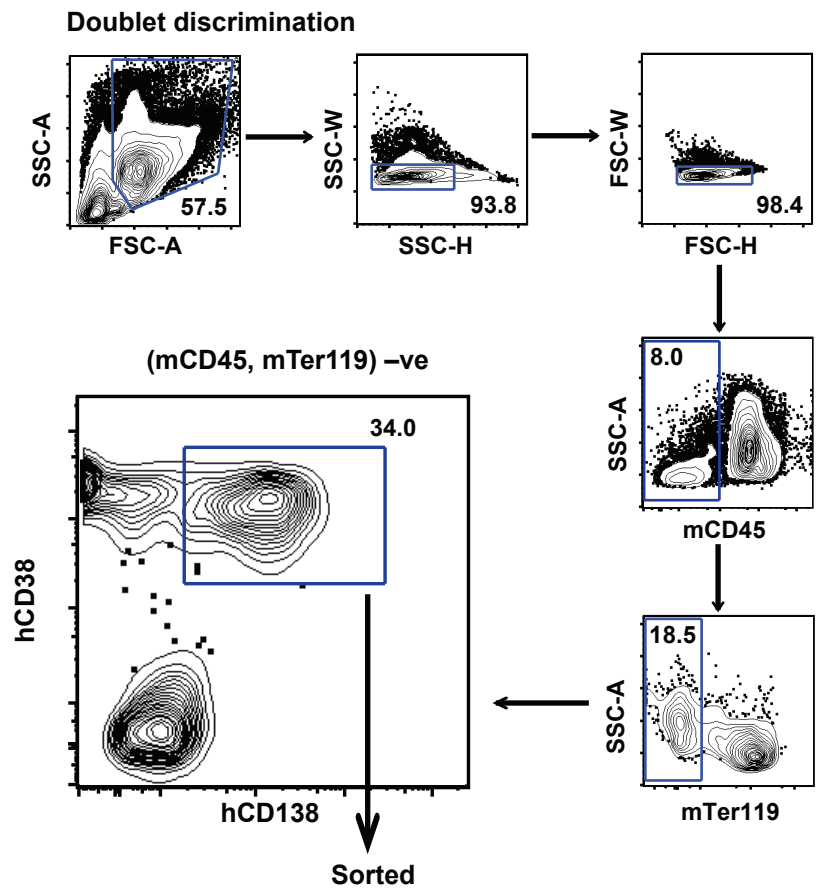
d)



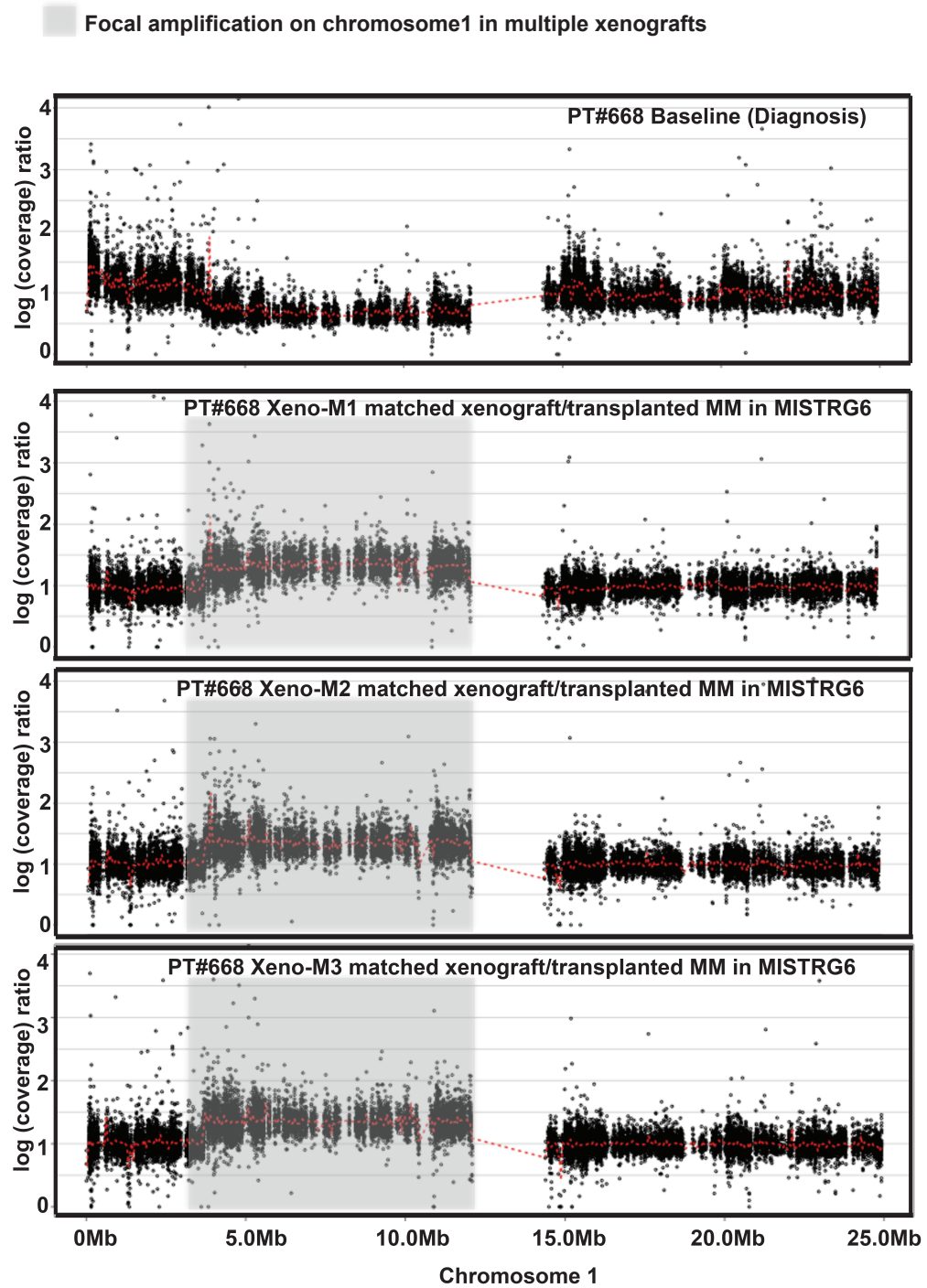
Supplementary Figure S3



Supplementary Figure S4



Supplementary Figure S5





**Supplementary Table 1. Patient Characteristics**

<b>All patients (N = 30)</b>	<b>n (%)</b>
Median age	60
Male	17 (57%)
Multiple myeloma	20 (67%)
Plasma cell leukemia	3 (10%)
Asymptomatic myeloma	4 (13%)
MGUS	3 (10%)
Heavy chain type: IGG	20 (67%)
Heavy chain type: IGA	7 (24%)
Heavy chain type IGD	1 (3%)
Light chain disease only	2 (6%)
Light chain type: kappa	20 (67%)

**Supplementary Table 2. Summary statistics for whole exome sequencing analysis.**

	<b>Germline samples</b>	<b>Tumor samples</b>
<b>SE/PE</b>	PE	PE
<b>Read length</b>	74bp	74bp
<b># of reads per lane (M)</b>	87.5	202.0
<b>Median coverage (X)</b>	64.3	147.6
<b>% of reads mapped on genome</b>	91.1%	90.7%
<b>% of reads mapped on target</b>	60.1%	59.1%
<b>% of targeted bases covered at least 8x</b>	96.6%	98.3%
<b>% of targeted bases covered at least 20x</b>	89.1%	96.5%
<b>% of targeted bases covered at least 50x</b>	62.4%	88.3%

**Supplementary Table 3. Source, clone and dilutions for antibodies**

<b>Flow cytometry</b>				
<b>Antibody against</b>	<b>Species reactivity</b>	<b>Source</b>	<b>Clone</b>	<b>Dilutions</b>
CD138	Human	BD Pharmingen	MI15	1:50
CD19	Human	BD Horizon	SJ25-C1	1:50
CD3	Human	Biologend	UCHT1	1:100
CD38	Human	BD Horizon	HIT2	1:500
CD45	Human	BD Pharmingen	HI30	1:100
CD45	Mouse	BD Pharmingen	30-511	1:400
CD56	Human	Biologend	HCD56	1:800
IgLambda	Human	Biologend	MHL-38	1:100
IgKappa	Human	Biologend	MHK-49	1:20
Ter119	Mouse	BD Pharmingen	TER-119	1:400
<b>Mass cytometry</b>				
<b>Antibody against</b>	<b>Species reactivity</b>	<b>Source</b>	<b>Clone</b>	<b>Dilutions</b>
CD11b	Human	Fluidigm	ICRF44	1:100
CD11c	Human	Fluidigm	Bu15	1:100
CD117	Human	Fluidigm	104D2	1:100
CD138	Human	Biologend	MI15	1:100
CD14	Human	Fluidigm	RMO52	1:100
CD16	Human	Biologend	3G8	1:100
CD185	Human	Biologend	J25D4	1:100
CD19	Human	Fluidigm	HIB19	1:100
CD25	Human	Fluidigm	2A3	1:100
CD274	Human	eBiosciences	MIH1	1:100
CD276	Human	Biologend	MIH42	1:100
CD3	Human	Fluidigm	UCHT1	1:100
CD33	Human	Fluidigm	WM53	1:100
CD38	Human	Fluidigm	HIT2	1:100
CD4	Human	Fluidigm	RPAT4	1:100
CD45	Human	Fluidigm	HI30	1:100
CD45	Mouse	Fluidigm	30-F11	1:100
CD56	Human	BD Pharmingen	HCD56	1:100
CD8	Human	Fluidigm	RPAT8	1:100
CD95	Human	Fluidigm	DX2	1:100
FoxP3	Human	Fluidigm	PCH101	1:100
HLA-DR	Human	Biologend	L243	1:100
IgLambda	Human	Fluidigm	MHL-38	1:100
IgKappa	Human	Fluidigm	MHK-49	1:100
Ki-67	Human	Fluidigm	Ki-67	1:100
Ter-119	Mouse	Fluidigm	TER-119	1:100
TIM-3	Human	Fluidigm	F38-2E2	1:100